2019 European Conference on Computing in Construction
Chania, Crete, Greece
July 10-12, 2019

BIM-DRIVEN MISSION PLANNING AND NAVIGATION FOR AUTOMATIC INDOOR CONSTRUCTION PROGRESS DETECTION USING ROBOTIC GROUND PLATFORM

Amir Ibrahim[1], Ali Sabet[2], and Mani Golparvar-Fard[1]
[1]University of Illinois at Urbana Champaign, United States of America
[2]University of Waterloo, Canada

Abstract

Reconstructing a complete and accurate 3D representation of indoor construction scenes is an important step towards automated visual monitoring of construction projects. For fast access to construction's as-built visual data, construction drones are programmed to autonomously navigate the outdoor space and collect the data. However, due to limited satellite signal indoors, ground rovers provide safer and more reliable autonomous navigation in the narrow cluttered indoor space. In this paper we present a novel pipeline for 4D BIM-driven mapping of the as-built state of indoor construction site. 2D Light Detection and Ranging (LiDAR) sensors are mounted on an Unmanned Ground Vehicle (UGV) for Simultaneous Localization and Mapping (SLAM). The developed method consists of (1) BIM-driven data collection planning; (2) automatic mission navigation; (3) LiDAR data collection and (4) dynamic obstacle avoidance. Experiments show the applicability of the developed data collection strategy and the improved safety of automatic mission execution using UGVs.

Introduction

Reality visual data is commonly collected to document the as-built state of construction site and provide clear communication between project parties (Golparvar-fard et al. 2012). Various devices are utilized to collect construction visual data. Hand-held cameras and mobile phones are commonly used by site personnel or hired professionals to collect informative images and videos. Stationary Pan-Tilt-Zoom (PTZ) cameras are installed on the job-site or mounted on tower cranes for real-time access to construction visual feed. Recently, remote controlled unmanned aerial vehicles (UAVs) are operated manually by drone pilots or automatically using drone mapping software to manually create visual data collection plans. These data collection plans aim to collect data that visually cover the constructed structure vertically and horizontally.

Construction progress reporting requires fast access to visual data frames that observes changes in the constructed structure at expected progress locations to detect the construction progress. The state-of-practice manual methods for videos and images collection are very slow and do not guarantee visual coverage to the locations of expected progress. Adding to that, the raw collected visual data requires cumbersome and resource intensive visual analysis tasks to organize and localize the data.

High end laser scanners are used to provide more accurate and complete as-built geometry of the job-site, these devises can collect dense and accurate 3D reality models using time-of-flight technology. The resulted pointcloud data is organized temporally and aligned with as-planned BIM models to visually communicate and analyze the construction progress. However, collecting reality data using laser scanners is associated with the challenges of:

- *Manual data collection planning* which is slow and inefficient as the fast pace of construction progress requires high frequency data collection planning to define scanning configurations according to the locations of expected changes.
- *No visual quality feedback* that is needed to assure complete visual coverage to the in-progress elements.
- *Inaccurate execution* of the data collection plan due to poor communication of the collection plan or inability to localize the laser scanner on the job-site.
- *Registration of local scans* that requires placement of visual tags at specific locations before scanning leading to extra costs, increased data collection duration and additional post-collection tasks.
- *High investment costs* associated with purchasing or renting the scanning devices and hiring professionals to operate the devices and analyze the data.

To overcome such challenges, automated data collection platforms -for instance ground rovers- are investigated for fast and accurate retrieval of construction visual data. Recently, several reports showed an increase in the adoption of construction drones in order to automate outdoors visual data collection (Drone Deploy 2018, Skyward 2018). Using Global Navigation Satellite System (GNSS), drones can automatically navigate waypoints according to the manually planned missions to collect the data. However, the limited GNSS signal and the narrow cluttered indoor

DOI:10.35490/EC3.2019.195

construction environment reduce the accuracy of localization and increase the risks of mid-air collisions. On the other hand, Unmanned Ground Vehicles (UGVs) are more reliable for indoor data collection due to the aforementioned collision risks. Adding to that, these platforms can be programmed for dynamic obstacle avoidance to prevent collision with moving objects on the job-site. UGVs have also higher payload capacity allowing them to carry multiple visual sensors that are needed to improve the accuracy of autonomous navigation and provide a variety of as-built data.

Related Works

Automatic progress detection requires accurate geometric representation of the as-built geometry of the construction site. State-of-the-art methods utilize the daily collected images and videos to reconstruct 4D reality models using Structure-from-Motion (SfM) algorithm (Schönberger & Frahm 2016). SfM algorithm outputs a colored pointcloud model that can be used as-is or converted to a meshed model using Poisson surface reconstruction (Kazhdan et al. 2006) for better interpretation of the data. Geometries of the reality models are compared with that of the as-planned 4D BIM to detect construction progress (Golparvar-fard et al. 2012).

To assure the accuracy of geometry-based progress detection, the visual quality of the collected data has to be evaluated before execution. However, state-of-practice data collection planning approaches do not provide visual quality feedback leading to bad quality of the collected data. Bad quality visual data results in incomplete and inaccurate 3D reconstructed models (Ibrahim, Golparvar-Fard, Bretl & El-Rayes 2017). These challenges are only reported after post-processing of the collected data and reconstructing the 3D as-built geometries. To improve the visual quality of the data and shorten their acquisition duration, change-driven visual quality metrics are utilized to provide visual quality feedback for the data collection plans before execution (Ibrahim, Roberts, Golparvar-Fard & Bretl 2017).

Light Detection and Ranging (LiDAR) sensors are also used to collect high quality 3D as-built geometries. Such sensors are utilized to directly collect dense and accurate reality pointcloud models relying on hardware capabilities. LiDAR data collection plans are defined by specifying locations and configurations of the sensor inside the construction site. The data collection plans aim to provide full 3D mapping of the construction site to record the state of progress (Zhang et al. 2016).

However, collecting LiDAR data still requires manual relocation and readjustment of the LiADR platform several times to place the device at the planned scanning locations. So in order to improve the speed and the quality of the data collection process, autonomous unmanned vehicles are being investigated to accurately execute the data collection plan and automatically collect the as-built visual data. These autonomous platforms can be categorized -according to their navigation strategies- into (1) GNSS-based platforms and (2) SLAM-based platforms.

GNSS-based platforms

Global Navigation Satellite System (GNSS) is used to localize the autonomous platform by triangulating the position of the mounted GNSS receiver with respect to multiple detected satellites. Such technology is mainly used for outdoor data collection using camera-equipped drones (Tahar & Kamarudin 2016, Ibrahim, Roberts, Golparvar-Fard & Bretl 2017, Rakha & Gorodetsky 2018, Freimuth & König 2018) or multi-sensory autonomous ground rovers (Kim et al. 2003, Ramanagopal & Ny 2016, Haala et al. 2008, Srinivasan Ramanagopal et al. 2018). To improve the accuracy of localization and mapping, fiducial tags are usually placed at pre-defined locations to provide ground truth survey points.

SLAM-based platforms

Simultaneous Localization and Mapping (SLAM) pipeline is used to create a map of the environment -2D or 3D- and concurrently estimate the location of the robotic platform relative to the map. For instance, Hector SLAM (Kohlbrecher et al. 2013) uses 2D LiDAR to build a navigation map and Iterative Closest Point (ICP) algorithm (Censi 2008) to detect the location of the LiDAR relative to the map. ORB SLAM (Mur-Artal et al. 2015) uses a monocular camera to detect the 3D locations of binary visual features and localize the camera with respect to these features through Visual Odometry (VO). SLAM algorithms are mainly used for indoor navigation due to limited GNSS signal indoors. However, SLAM is associated with drift errors leading to geometrical inconsistencies in the reconstructed map and incremental localization errors. To reduce the errors, several sensors -as wheels odometers and internal measurement units- are fused with VO to improve the platform's state estimate using Extended Kalman Filter (EKF) (Einicke & White 1999) for fused state estimation.

A prior model or a 3D representation of the construction scene is required for creating and evaluating a data collection plan. A visual quality feedback during data collection planning assures good visual coverage to the in-progress elements. Taneja et al. (2016) defined BIM-based indoors navigation models using Industry Foundation Classes (IFC) that stores the model's geometric information and the relationship between the model's elements. These networks can be used for indoors localization given that the utilized BIM has high level of details (LOD) and is up-to-date. Hover et al. (2012) used low resolution models to plan for complete high resolution mapping of a ship-hull using visual and acoustic sensors. Jing & Shimada (2018), Baik & Valenzuela (2018) used simple geometric models to represent the structure's topography and thus enable planning for complete visual coverage of the structure using camera-equipped drone. Ibrahim, Roberts, Golparvar-Fard & Bretl (2017) used 4D BIM model to create and simulate flight plans for outdoors data collection. Nevertheless, other methods are developed for navigation without a prior model, for instance exploration policies are used to automatically navigate a robotic platform in the unknown space (Taylor & Kriegman 1995, Ramanagopal & Ny 2016). However, exploration-based navigation methods are not tailored for construction change-driven data collection planning and thus not considered in this research.

Collection Platform

In this research, we used a Clearpath Jackal ground rover for automated indoors data collection. The rover is equipped with wheels odometer and an IMU for supporting accurate localization. To reduce the overall cost of the collection platform, two 2D LiDARs are mounted orthogonal to each other for accurate mapping and navigation as shown in Figure 1. The first LiDAR has longer range (16 meters) installed horizontally to create 2D occupancy grid map used for navigation. The second LiDAR has shorter range (10 meters) and oriented vertically to create cross section scans of the structure during navigation. The ground robot also provides the following capabilities:

- Large payload capacity that allows the installation and fusion of multiple sensors
- Good computational power with the high performance on-board computer
- Dynamic obstacle avoidance and safer operation with stop in-place fail safe strategy
- Longer operating duration with a battery that can last for 2 $\sim$ 3 hours

Data Collection Pipeline

Hector SLAM Kohlbrecher et al. (2011) algorithm was chosen for localization and navigation due to the lack of GNSS signal inside the constructed structure. Hector SLAM utilizes sensory observations from the long range LiDAR to create an accurate and high resolution 2D occupancy grid map. The map is initialized with cells (grid) marked as unknown and then each cell is identified as empty or occupied by detecting fixed obstacles around the robot while it is in motion. For each horizontal 360°scan, the scan points are matched against the global occupancy map using Iterative Closest Point (ICP) algorithm to detect the configuration of the sensor (location and orientation). The estimated configuration is then used to transform the latest scan points to the global map frame for updating the global occupancy map in real-time.

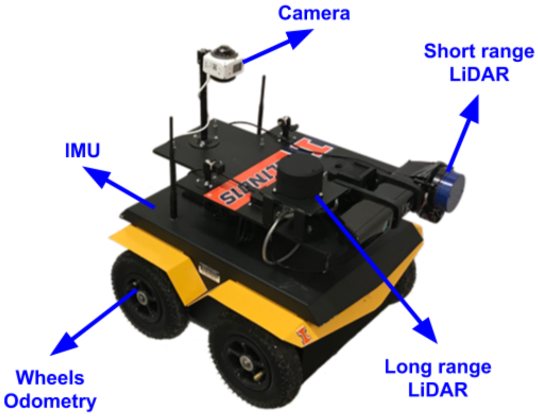

Figure 1: The indoors robotic collection platform

To create 3D pointcloud model, the rover navigates the data collection path automatically using pre-defined waypoints. Each new vertical scan retrieved from the LiDAR is converted to pointcloud and then registered to the global pointcloud using the synchronized robot pose calculated using Hector SLAM localization module (Figure 2). To synchronize the LiDAR data with the robot's pose, time stamps associated with the scan data and the robot pose estimation are used. Where the time stamp of each observed scan data (message) is used to query for the robot pose with the same time stamp. If the queried time stamp lies between two successive poses, the accurate pose is retrieved by interpolating the translation and rotation values of the two poses. Adding to that, when the rover reaches a waypoint, it performs a 360°in-place rotation to assemble 2D vertical scans into 3D pointcloud at the location of the waypoint.

To enable automatic navigation, an initial navigation map - occupancy grid map- has to be created manually by driving the ground robot inside the indoors space. After the space is mapped completely, the occupancy grid map is saved to be used for future mission planning. The initial map is also used for automatic navigation by localizing the robot with respect to navigation waypoints that are defined inside initial map. Details of planning and autonomous navigation are discussed in the following sections.

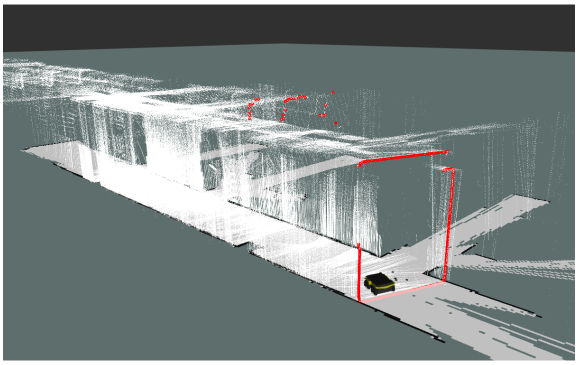

Figure 2: Vertical scan points displayed with red color registered to the global pointcloud colored in white

Planing

Model-driven data collection planning is utilized to define waypoints that visually observe the locations of expected changes. 4D BIM is used to identify such locations by color coding the elements with expected progress and creating navigation waypoints close to these elements. Since the plan's waypoints are defined in 2D, a 2D floor plan is retrieved from the BIM model by creating a cross section at the data collection floor. The user then defines the locations and orientations of the waypoints preferably in the middle of each room/space that contains in-progress elements.

To transform the data collection plan to the navigation map's coordinates, a 2D transformation matrix is calculated through manual registration of the 2D floor plan and the navigation map. During the registration process, the user defines pairs of points -at least two- that create correspondences between the floor plan and the navigation map. The corresponding points are used to solve for the translation, rotation and scale parameters that are then used to transform all waypoints from the 2D floor plan frame to the navigation map frame. The transformed collection plan is then uploaded to the rover's on-board computer and executed on the job-site.

Autonomous Navigation

Given the initial navigation occupancy grid map and the transformed waypoints, LiDAR-based SLAM is used to localize the robot in the occupancy grid map. A path planner is used to define a navigable path between the robot's current configuration and each waypoint successively using A* algorithm (Hart et al. 1967). The A* algorithm uses heuristics-based search to detect the shortest path along the unoccupied cells of the map connecting between the robot's location and the location of each waypoint. The robot then navigates the defined path using the mounted Micro Controller (MC) unit that controls the wheels' rotation to drive the robot according to the planned path.

Obstacle Avoidance

Due to the presence of dynamic obstacles on the job-site -for instance moving personnel-, a local path planner is used to locally alter the global planned path. The local path planner uses the same A* heuristics to create detours along the main path to navigate around the obstacles. A local occupancy grid map with finer resolution is used for high frequency detection and avoidance of obstacles. The user also defines a safe offset distance that inflates the obstacles' footprint in the navigation map to avoid unexpected collisions resulting from localization errors. An escape policy is also defined to drive the robot away from moving obstacle in case an obstacle is moving towards the robot.

Experimental Setup and Results

The introduced indoors data collection pipeline is tested using the data collection robotic platform. Robot Operating System (ROS) framework (Quigley et al. 2009) is installed on the robot's on-board computer to communicate the robot's state estimate, the observed sensory data and the developed algorithms in real-time. The framework also sends navigation actions to the robot's Micro Controller (MC) unit for mission execution. Stitching local vertical LiDAR scans and transforming them to 3D reality model is developed and integrated with ROS as part of this research. Hector SLAM, autonomous navigation and dynamic obstacle avoidance modules are integrated using open source software packages available online.

Two indoors experiments were conducted to (1) validate the applicability of the developed pipeline; (2) evaluate the safety of autonomous execution; and (3) assess the quality of the reconstructed 3D reality model in terms of density and accuracy of the model.

The first experiment was conducted in a structural university lab. The lab simulates a cluttered indoors construction space with the presence of built-up structural elements, small equipment and personnel. An initial occupancy map (Figure 3) was created manually by driving the robot around the lab. The collected reality model is then retrieved and visualized in Reconstruct web platform that offers 3D visualization of BIM and reality models (Figure 4). The dynamic obstacle avoidance module was tested by having a person walk in front of the robot while executing a simple two waypoints autonomous mission.

After testing the platform in the lab and ensuring its safe operation, a second experiment was conducted on a real construction site. Adding to that, data collection operation was performed after working hours to mitigate any interference between the autonomous mission execution

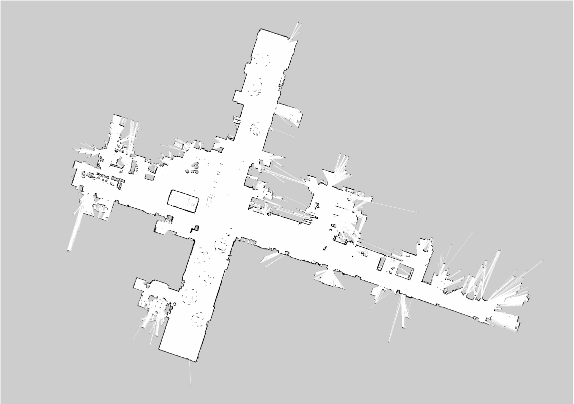

Figure 3: Occupancy grid map collected for the first experiment

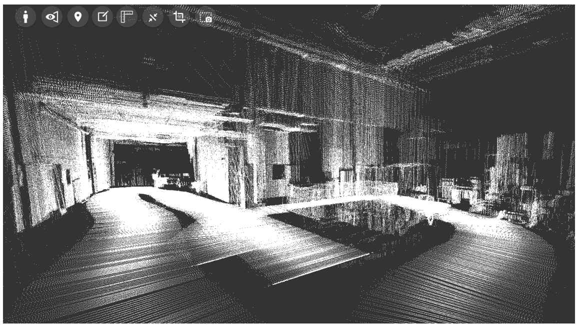

Figure 4: Collected Reality pointcloud model for the structural lab

and the on going construction work. The platform was deployed to collect reality model on the second floor of a building during indoors partitioning construction phase. The floor is composed of a long corridor connecting 10 residential units. An initial occupancy grid map was created manually and then used to navigate the ground robot to collect data. Data collection plan was defined using the 2D floor plan of the building visualized using Reconstruct web platform. The data collection waypoints are placed manually to navigate the robot through 20 waypoints -two waypoints per unit- to collect reality data covering the in-progress elements. Using Reconstruct platform, the 2D floor plan was registered to the occupancy map by manually picking six corresponding points that align the floor plan with the occupancy map. The retrieved transformation matrix from the previous step is used to transform the 20 waypoints from the BIM Cartesian coordinates to the navigation map frame (Figure 5).

The collected pointcloud data is then evaluated for quality by measuring the density and accuracy of the points. The density of the model at a specific location is measured by counting the number of neighboring points within a unit surface area at that location. The later calculation is conducted for each point's location of the reality model and the distribution of the density across the model is reported (Figure 6). For accuracy calculation, the reality model is registered with the project's BIM model (Figure 7), and the distance between each point and the closest BIM element is used to measure the accuracy.

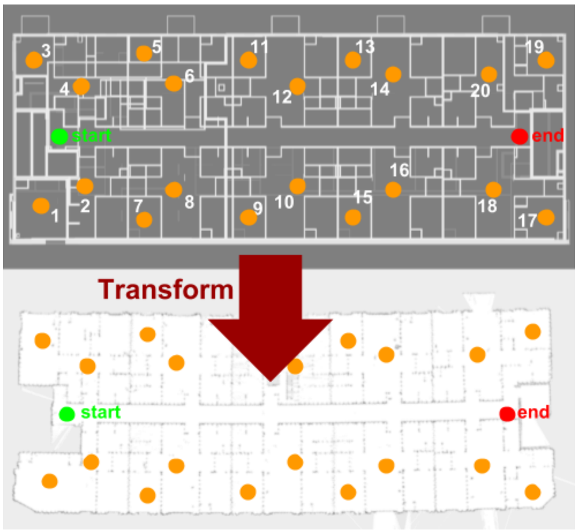

Figure 5: Transformed waypoints from 2D BIM floor plan at the top to the navigation map at the bottom

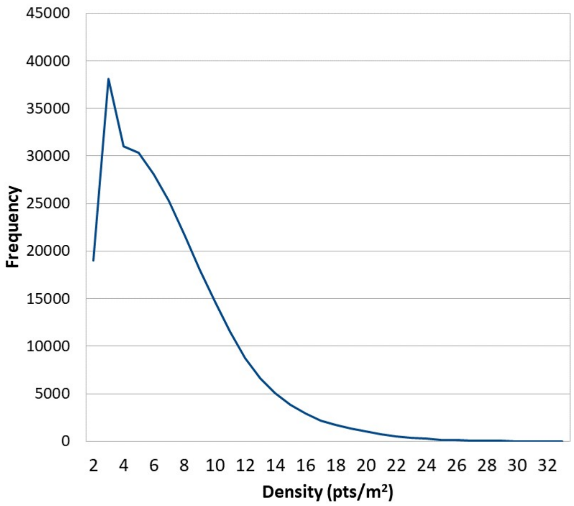

Figure 6: Density distribution for the reality model collected in experiment 2

Evaluation of the model's density reported a mean density of 6.85 pts/m^2 with 4.05 pts/m^2 standard deviation and 6 pts/m^2 median. Evaluating the model's accuracy reported a mean accuracy of 0.51 m with 0.65 m standard deviation and 0.3 m median. Also, results show that locations with

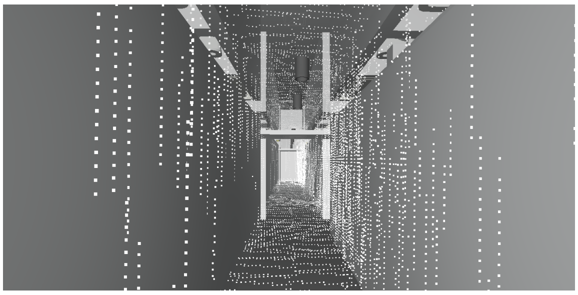

Figure 7: Pointcloud model collected for the second experiment and overlaid on BIM model for visualization

high density results in better accuracy detected through improvements in the mean and standard deviation of the measured accuracy (Figure 8).

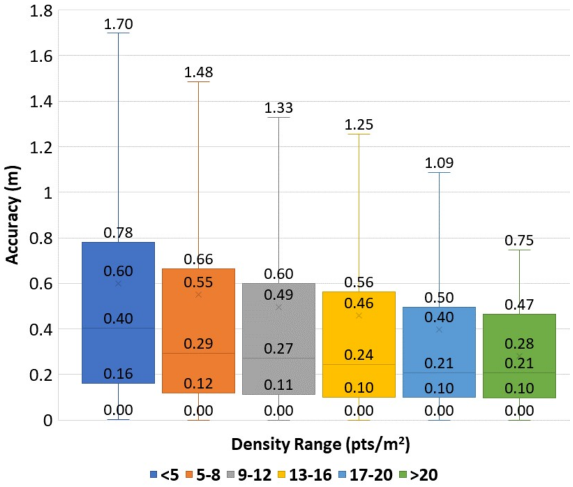

Figure 8: Distribution of reality model's accuracy with respect to points density

The results also show that the low detected density and accuracy of the reality model are affected by:

- The low resolution and accuracy associated with the utilized 2D LiDAR device. The choice of such LiDAR was a compromise to reduce the overall cost of the collection platform.
- The few number of waypoints and manual placement of the waypoints result in poor visual coverage to some regions on the constructed floor.
- Placement of waypoints in the middle of rooms to improve visual coverage and navigation safety resulted in lower density of points associated with far walls as the spacing between the scanned points increases with the distance.
- Drift errors associated with the SLAM pipeline led to incorrect registration of some local points to the global pointcloud model.
- Utilizing manual registration of the pointcloud model with the BIM model led to lowering the model's accuracy due to registration errors.

Conclusions

In this paper we presented a novel pipeline for automated indoor data collection using LiDAR sensors mounted on an Unmanned Ground Vehicle. The developed pipeline utilizes 4D BIM-driven data collection planning to define waypoints that capture the as-built state of the job-site at the locations of expected progress. LiDAR-based SLAM is used for localization and navigation by constructing an accurate and high resolution pointcloud map. To enable automatic navigation, an initial navigation map is created by manually driving the robotic platform. The initial map is then used for automatic navigation to follow user-defined data collection waypoints localized in the map's coordinate system.

A 2D LiDAR sensor is mounted vertically on the ground robot to collect 2D cross section scans of the indoor space during autonomous navigation. the cross section scans are converted to local pointclouds that are registered to a global pointcloud map using the synchronized pose of the sensor. During autonomous mission execution, the robot navigates the shortest safe path between waypoints while collecting data. Adding to that, at each waypoint the robot performs a 360°in-place rotation to create a 3D model from the cross section scans.

Results from the first experiment show the applicability of the framework for safe indoors navigation while dynamically avoiding moving obstacle. The experiment also shows the scalability of Hector SLAM for mapping large indoor construction spaces and the usability of the resulting occupancy map for autonomous navigation. The second experiment reported the quality of the reconstructed pointcloud model with a mean density of 6.85 points per m^2 and mean accuracy of 0.51 m. It was also observed that locations with higher pointcloud density are associated with improved accuracy.

Future work will focus on automating the process of indoor mission planning to further reduce the duration of data acquisition. Visual quality evaluation will be conducted before data collection execution to assure complete visual coverage of in-progress elements and improve the quality of the reconstructed reality model. To provide semantic information for the collected pointclouds, frames captured from a mounted omnidirectional camera will be used to color the scanned points. In addition, the accuracy of collected pointcloud model will be improved by using fiducial tags to reduce drift errors.

Acknowledgements

This material is based in part upon the work supported by the National Science Foundation under Grant CMMI 1446765. Any opinions, findings, and conclusions or recommendations expressed in this material are those of the author(s) and do not necessarily reflect the views of the National Science Foundation.

References

Baik, H. & Valenzuela, J. (2018), ‘Unmanned Aircraft System Path Planning for Visually Inspecting Electric Transmission Towers’, *Journal of Intelligent & Robotic Systems* .

Censi, A. (2008), An ICP variant using a point-to-line metric, *in* ‘2008 IEEE International Conference on Robotics and Automation’, Pasadena, CA, USA.

Drone Deploy (2018), Commercial Drone Industry Trends, Technical report.

Einicke, G. A. & White, L. B. (1999), ‘Robust Extended Kalman Filtering’, *IEEE TRANSACTIONS ON SIGNAL PROCESSING* **47**(9), 2596–2598.

Freimuth, H. & König, M. (2018), ‘Planning and executing construction inspections with unmanned aerial vehicles’, *Automation in Construction* **96**, 540–553.

Golparvar-fard, M., Peña Mora, F. & Savarese, S. (2012), ‘Automated Progress Monitoring Using Unordered Daily Construction Photographs and IFC-Based Building Information Models’, *Journal of Computing in Civil Engineering* **29**(1).

Haala, N., Peter, M., Kremer, J. & Hunter, G. (2008), ‘Mobile Lidar Mapping for 3D Point Cloud Collection in Urban Areas a Performance Test’, *The International Archives of the Photogrammetry, Remote Sensing and Spatial Information Sciences* pp. 1119–1124.

Hart, P. E., Nilsson, N. J. & Raphael, B. (1967), ‘A Formal Basis of the Heuristic Determination of Minimum Cost Paths’, *IEEE Transactions of Systems Science and Cybernetics* **4**(2), 100–107.

Hover, F. S., Eustice, R. M., Kim, A., Englot, B. J., Johannsson, H., Kaess, M. & Leonard, J. J. (2012), ‘Advanced Perception, Navigation and Planning for Autonomous In-Water Ship Hull Inspection’, *Intl. J. of Robotics Research* **31**(12), 1445–1464.

Ibrahim, A., Golparvar-Fard, M., Bretl, T. & El-Rayes, K. (2017), Model-Driven Visual Data Capture on Construction Sites: Method and Metrics of Success, *in* ‘International Workshop for Computing in Civil Engineering (IWCCE 2017)’, pp. 109–116.

Ibrahim, A., Roberts, D., Golparvar-Fard, M. & Bretl, T. (2017), ‘An Interactive Model-Driven Path Planning and Data Capture System for Camera-Equipped Aerial Robots on Construction Sites’, *International Workshop for Computing in Civil Engineering (IWCCE 2017)* pp. 117–124.

Jing, W. & Shimada, K. (2018), ‘Model-based view planning for building inspection and surveillance using voxel dilation, Medial Objects, and Random-Key Genetic Algorithm’, *Journal of Computational Design and Engineering* **5**(3), 337–347.

Kazhdan, M., Bolitho, M. & Hoppe, H. (2006), Poisson Surface Reconstruction, *in* ‘Eurographics Symposium on Geometry Processing’.

Kim, S.-k., Russell, J. S. & Koo, K.-j. (2003), ‘Construction Robot Path-Planning for Earthwork Operations’, *Journal of Computing in Civil Engineering* **17**(2), 97–104.

Kohlbrecher, S., Meyer, J., Graber, T., Petersen, K., Klingauf, U. & Von Stryk, O. (2013), ‘Hector open source modules for autonomous mapping and navigation with rescue robots’, *Behnke S., Veloso M., Visser A., Xiong R. (eds) RoboCup 2013: Robot World Cup XVII. RoboCup 2013. Lecture Notes in Computer Science* **8371 LNAI**, 624–631.

Kohlbrecher, S., Von Stryk, O., Meyer, J. & Klingauf, U. (2011), ‘A flexible and scalable SLAM system with full 3D motion estimation’, *9th IEEE International Symposium on Safety, Security, and Rescue Robotics, SSRR 2011* pp. 155–160.

Mur-Artal, R., Montiel, J. M. & Tardos, J. D. (2015), ‘ORB-SLAM: A Versatile and Accurate Monocular SLAM System’, *IEEE Transactions on Robotics* **31**(5), 1147–1163.

Quigley, M., Gerkey, B., Conley, K., Faust, J., Foote, T., Leibs, J., Berger, E., Wheeler, R. & Ng, A. (2009), ‘ROS: an open-source Robot Operating System’, *ICRA Workshop on Open Source Softwar* .

Rakha, T. & Gorodetsky, A. (2018), ‘Review of Unmanned Aerial System (UAS) applications in the built environment: Towards automated building inspection procedures using drones’, *Automation in Construction* **93**(September), 252–264.

Ramanagopal, M. S. & Ny, J. L. (2016), ‘Motion Planning Strategies for Autonomously Mapping 3D Structures’, *arXiv:1602.06667* pp. 1–11.

Schönberger, J. L. & Frahm, J.-M. (2016), 'Structure-from-Motion Revisited', *IEEE Conference on Computer Vision and Pattern Recognition (CVPR)* .

Skyward (2018), State of Drones in Big Business, Technical report.

Srinivasan Ramanagopal, M., Nguyen, A. P. V. & Le Ny, J. (2018), 'A Motion Planning Strategy for the Active Vision-Based Mapping of Ground-Level Structures', *IEEE Transactions on Automation Science and Engineering* **15**(1), 356–368.

Tahar, K. N. & Kamarudin, S. S. (2016), UAV onboard GPS in positioning determination, *in* 'The International Archives of the Photogrammetry, Remote Sensing and Spatial Information Sciences', Vol. XLI-B1, pp. 1037–1042.

Taneja, S., Akinci, B., Garrett, J. H. & Soibelman, L. (2016), 'Algorithms for automated generation of navigation models from building information models to support indoor map-matching', *Automation in Construction* **61**, 24–41.
URL: *http://dx.doi.org/10.1016/j.autcon.2015.09.010*

Taylor, C. J. & Kriegman, D. J. (1995), 'Vision-based motion planning and exploration', *Algorithmic Foundations of Robotics* **14**(3), 69–83.

Zhang, C., Kalasapudi, V. S. & Tang, P. (2016), 'Rapid data quality oriented laser scan planning for dynamic construction environments', *Advanced Engineering Informatics* **30**(2), 218–232.